

Persistent Pulmonary Nodular Ground-Glass Opacity at Thin-Section CT: Histopathologic Comparisons¹

Ha Young Kim, MD
Young Mog Shim, MD
Kyung Soo Lee, MD
Joungho Han, MD
Chin A Yi, MD
Yoon Kyung Kim, MD

Purpose:

To retrospectively compare pure pulmonary ground-glass opacity (GGO) nodules observed on thin-section computed tomography (CT) images with histopathologic findings.

Materials and Methods:

The institutional review board approved this study and waived informed consent. Histopathologic specimens were obtained from 53 GGO nodules in 49 patients. CT scans were assessed in terms of nodule size, shape, contour, internal characteristics, and the presence of a pleural tag. The findings obtained were compared with histopathologic results. Differences in thin-section CT findings according to histopathologic diagnoses were analyzed by using the Kruskal-Wallis test or Fisher exact test.

Results:

Of 53 nodules in 49 patients (20 men, 29 women; mean age, 54 years; range, 29–78 years), 40 (75%) proved to be bronchoalveolar cell carcinoma (BAC) ($n = 36$) or adenocarcinoma with predominant BAC component ($n = 4$), three (6%) atypical adenomatous hyperplasia, and 10 (19%) nonspecific fibrosis or organizing pneumonia. No significant differences in morphologic findings on thin-section CT scans were found among the three diseases (all $P > 0.05$). A polygonal shape (25%, 10 of 40 nodules) and a lobulated or spiculated margin (45%, 18 of 40) in BAC or adenocarcinoma with predominant BAC component were caused by interstitial fibrosis or infiltrative tumor growth. A polygonal shape and a lobulated or spiculated margin were observed in two (20%) and three (30%) of 10 nodules, respectively, in organizing pneumonia/fibrosis were caused by granulation tissue aligned in a linear manner in perilobular regions with or without interlobular septal thickening.

Conclusion:

About 75% of persistent pulmonary GGO nodules are attributed to BAC or adenocarcinoma with predominant BAC component, and at thin-section CT, these nodules do not manifest morphologic features that distinguish them from other GGO nodules with different histopathologic diagnoses.

© RSNA, 2007

¹ From the Department of Radiology and Center for Imaging Science (H.Y.K., K.S.L., C.A.Y., Y.K.K.), Department of Thoracic Surgery (Y.M.S.), and Department of Pathology (J.H.), Samsung Medical Center, Sungkyunkwan University School of Medicine, 50, Ilwon-Dong, Kangnam-Ku, Seoul 135-710, Korea. Received September 28, 2006; revision requested December 8; revision received December 13; accepted January 6, 2007; final version accepted March 19. Supported by the Korea Research Foundation Grant funded by the Korean Government (MOEHRD) (KRF-2005-042-D00246). Address correspondence to K.S.L. (e-mail: kyungs.lee@samsung.com).

Pulmonary subsolid nodules are defined as nodular areas of homogeneous or heterogeneous attenuation that are hypoattenuating with respect to surrounding soft-tissue structures such as vessels (1,2). Subsolid nodules can be further classified as either part-solid (in the case of nodules with patches of parenchyma that are completely obscured) or nonsolid (for nodules without such areas). Nonsolid pure ground-glass opacity (GGO) nodules, when persistently (either no change or an increase in diameter for ≥ 1 month) present on serial thin-section computed tomography (CT) scans, suggest the possibility of atypical adenomatous hyperplasia (AAH), bronchioalveolar cell carcinoma (BAC) (1–5), pulmonary lymphoproliferative disorder (6), or organizing pneumonia/fibrosis nodules (7).

Although persistent pure GGO nodules on thin-section CT scans represent BAC, AAH, lymphoproliferative disease, or organizing pneumonia/fibrosis, the percentages accounted for by these diseases are unknown. In addition, little has been reported on how BAC can be distinguished from the other diseases on thin-section CT images. According to one report, AAHs are less than 10 mm in diameter; however, others report that their diameters overlap those of BAC and AAH. In addition, GGO is an important constituent of lymphoproliferative disease and focal organizing pneumonia/fibrosis (6,7).

Although several articles (6,8) have reported on thin-section CT–pathologic

comparisons for pure GGO nodules, few reports are available for multiple pulmonary GGO nodules (9). Thus, the purpose of our study was to retrospectively compare pure pulmonary GGO nodules observed on thin-section CT images with histopathologic findings.

Materials and Methods

Our institutional review board (Samsung Medical Center, Sungkyunkwan University School of Medicine, Seoul, Korea) approved our retrospective study with a waiver of informed consent; written informed consent was acquired for the use of CT scans for all patients.

Patients

We (Y.M.S., K.S.L.) reviewed all surgical biopsy files recorded from November 1994 to August 2006, and selected studies with the descriptive term “GGO nodule” on CT reports and with tissue biopsy findings. Patients who had no lung biopsy and those who had a possible false-negative CT (ie, no GGO nodule described on radiologic report) were not included. A GGO nodule (solid portion is $\leq 5\%$ of nodule volume) was defined as a discrete pulmonary nodular abnormality 3 cm or less in diameter, with homogeneous attenuation that was not as high as that of surrounding soft-tissue structures (eg, blood vessels). The nodule had a diameter ratio of short and long axes within a factor of 1.5 of each other on transverse scans and was observed on a successive number of thin-section CT scans, thereby verifying that the lesion is spherical.

We also included studies with multiple GGO nodules with tissue confirmation for at least one of these multiple nodules. This study included a total of 49 patients with persistent (no change or an increase in diameter for ≥ 1 month) nodules at serial CT examinations. All patients under-

went at least one previous CT examination at least 1 month or more before this study. The 49 patients had a total of 127 pure GGO nodules. Thirty-seven patients had a single nodule and 12 had multiple nodules (one patient had two nodules, one had three nodules, two had four nodules, and eight had five or more nodules) at CT.

The CT-histopathologic comparison study included 53 nodules in 49 patients. One specimen was obtained from each of 37 patients with a single GGO nodule, from one of multiple GGO nodules in nine patients, from two of multiple nodules in two patients, and from three of multiple nodules in one patient.

Demographic Evaluation

Age, sex, history of cigarette smoking, the presence of respiratory symptoms, and prior lung or head and neck cancer or other risk factors for lung cancer were assessed (Y.M.S., K.S.L.). In addition, we also reviewed how these GGO nodules were detected (eg, incidental nodules on chest CT scans or identified nodules during lung cancer screening). The results of percutaneous needle aspiration biopsy and positron emission tomography were also recorded.

Image Acquisition and Analysis

Helical CT scans were obtained by using single-detector (eight patients with 14 nodules; HiSpeed Advantage, GE Healthcare, Milwaukee, Wis), four-detector

Advances in Knowledge

- Of 53 pure ground-glass opacity nodules, 40 (75%) were diagnosed as bronchioalveolar cell carcinoma (BAC) or adenocarcinoma with predominant BAC component, three (6%) as atypical adenomatous hyperplasia, and 10 (19%) as nonspecific organizing pneumonia/fibrosis.
- No morphologic features visualized at thin-section CT allowed these three diseases to be differentiated.

Implication for Patient Care

- No morphologic features visualized at thin-section CT allow for the differentiation of BAC or adenocarcinoma with BAC component from other diseases.

Published online

10.1148/radiol.2451061682

Radiology 2007; 245:267–275

Abbreviations:

AAH = atypical adenomatous hyperplasia
BAC = bronchioalveolar cell carcinoma
GGO = ground-glass opacity

Author contributions:

Guarantor of integrity of entire study, K.S.L.; study concepts/study design or data acquisition or data analysis/interpretation, all authors; manuscript drafting or manuscript revision for important intellectual content, all authors; approval of final version of submitted manuscript, all authors; literature research, all authors; clinical studies, all authors; statistical analysis, H.Y.K., Y.M.S., K.S.L.; and manuscript editing, H.Y.K., Y.M.S., K.S.L., J.H., C.A.Y.

Authors stated no financial relationship to disclose.

(24 patients with 59 nodules; LightSpeed QX/I, GE Healthcare), eight-detector (12 patients with 15 nodules; LightSpeed Ultra, GE Healthcare), or 16-detector (five patients with 39 nodules; LightSpeed16, GE Healthcare) row scanners. Scanning was performed from the thoracic inlet to the middle portion of the kidneys; unenhanced scans were obtained from eight patients for 50 nodules and both contrast material-enhanced and unenhanced scans from 41 patients for 77 nodules. For contrast-enhanced images, 100 mL of contrast medium (Iomeron 300;

Bracco, Milan, Italy) was administered intravenously.

In all patients, the scanning parameters were 120 kVp and 70–200 mA. Scanning and image reconstruction for single-detector row helical CT was performed with a section thickness of 7 mm, a pitch of 1, and a reconstruction interval of 7 mm; for 4–16-section CT, beam width of 10 mm, a beam of 1.375–1.5, and a reconstruction interval of 2.5–5.0 mm. For single-detector helical CT, additional thin-section (1.0–2.5-mm section thickness) CT scans were obtained from GGO nodules, whereas the 1.25–2.5-mm thin-section CT scans were acquired by using retrospective reconstruction of raw data for 4–16-section CT.

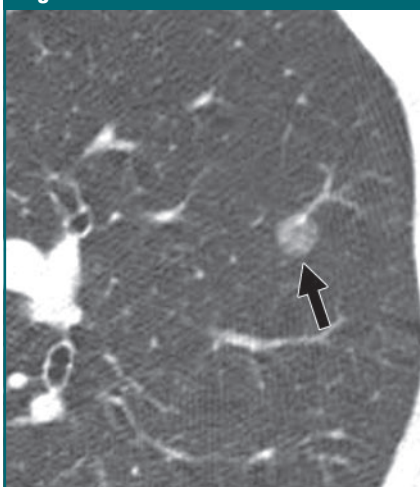
All image data were reconstructed by using a bone algorithm. Data were interfaced directly to our picture archiving and communication system (PathSpeed or Centricity 2.0; GE Healthcare, Mt. Prospect, Ill), which displayed all image data on monitors (four monitors, 1536 × 2048 matrix, 8-bit viewable

gray-scale, 60-foot-lambert luminescence). The monitors were used to view both mediastinal (width, 400 HU; level, 20 HU) and lung (width, 1500 HU; level, –700 HU) window images.

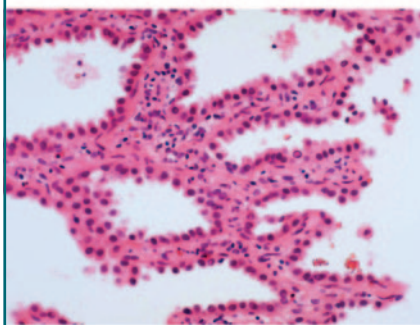
Two chest radiologists (H.Y.K., C.A.Y., with 2 and 5 years experience in chest CT, respectively), unaware of the clinical findings and histologic diagnoses of GGO nodules, assessed CT scans retrospectively. Decisions on CT findings were reached by consensus. CT scans were assessed by observing nodule size, shape, contour, internal characteristics, and the presence of a pleural tag.

The longest tumor diameters were measured. Shapes were classified as round, oval, or polygonal. Marginal characteristics were classified as smooth, lobulated, spiculated, or lobulated and spiculated. The presence of a bubble-like lucency or a pleural tag was recorded. Bubble-like lucency was defined as round or branching air attenuation in a GGO nodule. A pleural tag was defined as a linear attenuation heading toward the pleura or the major or minor

Figure 1



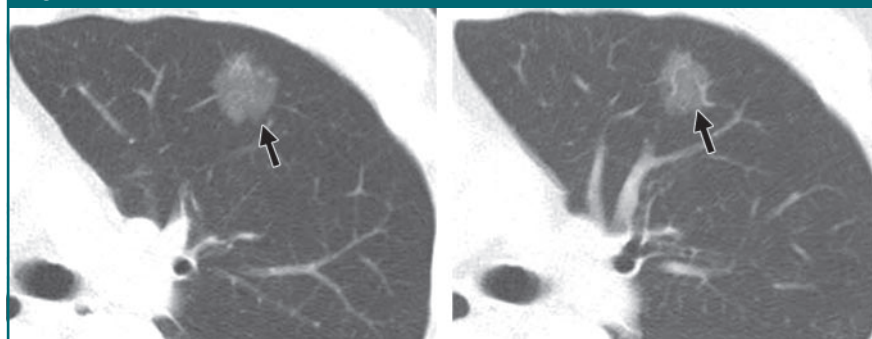
a.



b.

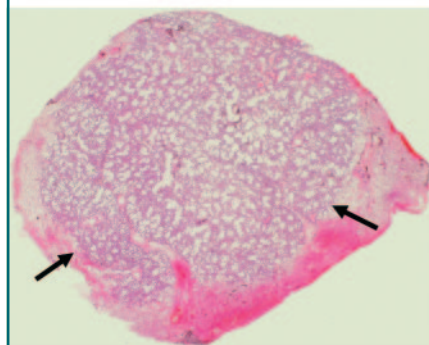
Figure 1: Nonmucinous BAC in 56-year-old asymptomatic woman. **(a)** Transverse lung-window thin-section (1.25-mm-thick) CT scan shows 8-mm round, well-defined GGO nodule (arrow) in left upper lobe. **(b)** Photomicrograph (hematoxylin-eosin stain; original magnification, ×100) shows columnar tumor cells growing along thickened alveolar walls (lepidic growth).

Figure 2



a.

b.



c.

Figure 2: Nonmucinous BAC in 63-year-old asymptomatic man. **(a, b)** Transverse lung-window thin-section (2.5-mm-thick, 10-mm interval) CT scans of distal left main bronchus show 22-mm GGO nodule (arrows) with slightly lobulated margin. **(c)** Photomicrograph (hematoxylin-eosin stain; magnification, ×1) shows round tumor (arrows) composed of uniform cuboid cell proliferations involving alveolar walls.

fissure from a GGO nodule. We also recorded the attenuation values of GGO nodules. A region of interest, ovoid or circular, covering one-half to two-thirds of the largest area in a GGO nodule away from areas of bubble-like lucency, was selected. For each GGO nodule, the average attenuation value (the mean of two measurements) and a standard deviation were calculated on unenhanced thin-section CT scans.

Because serial CT scans (for 53 nodules in 49 patients) were available in all patients (follow-up range, 1–78 months; mean, 10 months), interval changes for GGO nodules in terms of maximum diameter or the new appearance of a solid portion within a lesion were investi-

gated. The fates of patients were also assessed during the follow-up period.

CT-Pathologic Comparison

The interval between chest CT and pathologic evaluation ranged from 0 to 49 days (mean, 8 days). Pathologic specimens were obtained by using video-assisted thoracoscopic surgery wedge resection in 23 patients, lobectomy in nine, and open thoracotomy in 17. In the 23 patients who underwent wedge resection, needle localization of the nodule was made with CT guidance. With multiple nodules, the larger nodule within 2 cm of the pleura or the fissure was the target of wedge resection.

Entire sections of resected tissues were fixed in formalin and embedded in paraffin. Several 4- μ m-thick sections taken from the equator of lesions were hematoxylin-eosin stained and examined by using light microscopy. All tissue sections were interpreted by using an experienced lung pathologist (J.H., with 14 years experience in lung pathology). BAC was defined as a tumor exhibiting a pure broncholoalveolar growth pattern with an increase in thickness of alveolar septae and no evidence of stromal, vascular, or pleural invasion according to the revised World Health Organization histologic classification system (10).

Adenocarcinoma with predominant

Figure 3

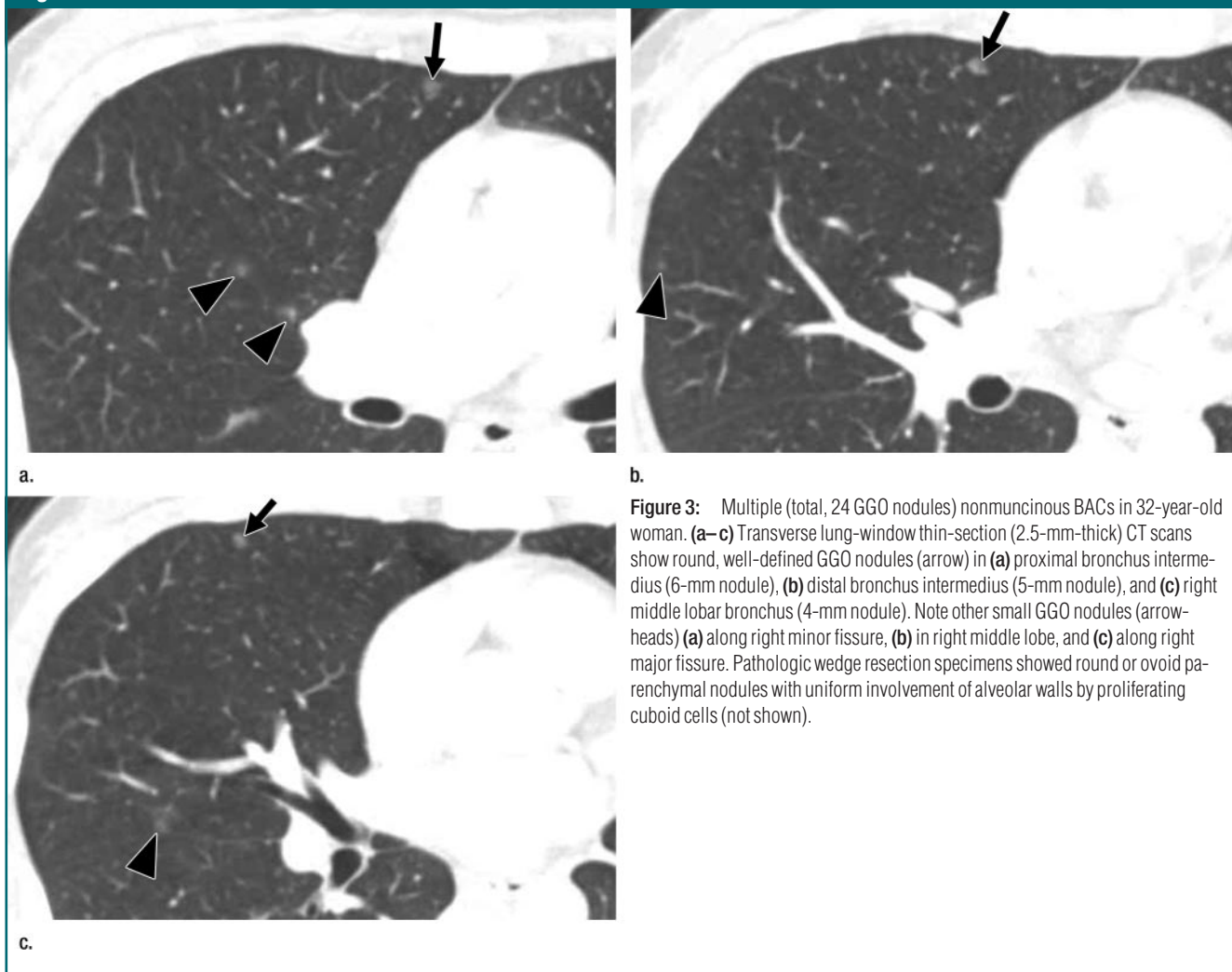


Figure 3: Multiple (total, 24 GGO nodules) nonmucinous BACs in 32-year-old woman. (a–c) Transverse lung-window thin-section (2.5-mm-thick) CT scans show round, well-defined GGO nodules (arrow) in (a) proximal bronchus intermedium (6-mm nodule), (b) distal bronchus intermedium (5-mm nodule), and (c) right middle lobar bronchus (4-mm nodule). Note other small GGO nodules (arrowheads) (a) along right minor fissure, (b) in right middle lobe, and (c) along right major fissure. Pathologic wedge resection specimens showed round or ovoid parenchymal nodules with uniform involvement of alveolar walls by proliferating cuboid cells (not shown).

BAC component was defined as a tumor demonstrating a BAC-like growth pattern with stromal invasive foci, which were considered present with several positive histologic parameters including fibroblastic proliferation, disruption of the elastic framework, and architectural distortion of the acinar or papillary structures by tumor cells. AAH was defined as a lesion with a well-defined boundary with alveoli and respiratory bronchioles that were lined by monotonous, slightly or minimally atypical cuboid to low-columnar epithelial cells with dense nuclear chromatin, inconspicuous nucleoli, and scant cytoplasm that did not elicit stromal thickening in alveolar septae (10). When diagnoses other than BAC or AAH were made, detailed histopathologic findings of hematoxylin-eosin-stained tissues were recorded.

The histopathologic-CT comparisons were examined for unusual morphologic features of GGO nodules, such as a polygonal shape, a lobulated or spiculated margin, and the presence of a pleural tag.

When lobectomy was performed in patients with BAC or adenocarcinoma with predominant BAC component (38 nodules in 24 patients), we also evaluated hilar or mediastinal nodal metastatic status.

Statistical Analysis

Statistical analyses were performed with SAS software (version 9.13; SAS Institute, Cary, NC). Patient demographics (ie, the ratio of men to women, GGO nodule multiplicity, the presence of respiratory symptoms, smoking history, and prior history of other malignancy) were compared with histopathologic diagnoses (eg, thin-nocarcinoma with predominant BAC component, AAH, and nonspecific fibrosis or organizing pneumonia) by using the Fisher exact test. Because BAC and adenocarcinoma with predominant BAC component had similar behavioral features and prognosis (6,9), they were put in the same group. Ages were compared by using the Kruskal-Wallis test.

Morphologic features regarding nodule size and attenuation values were compared with histopathologic diagnoses by

Figure 4

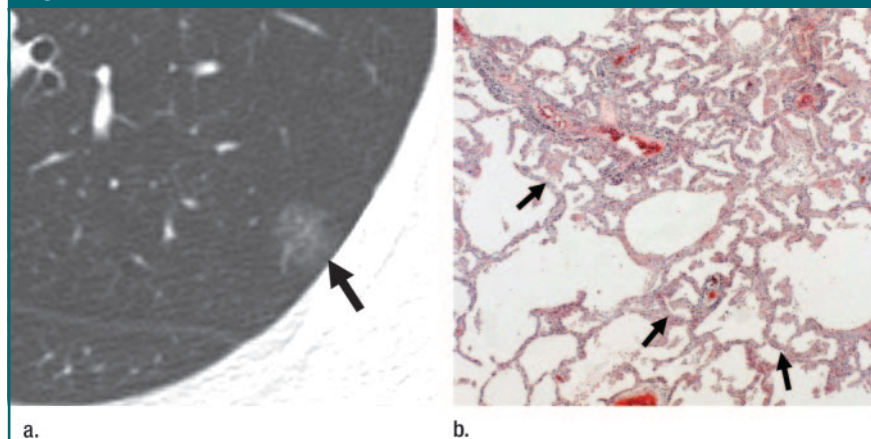


Figure 4: AAH in 55-year-old man. (a) Transverse lung-window thin-section (2.5-mm-thick) CT scan shows 12-mm round, well-defined GGO nodule (arrow) in left upper lobe. (b) Photomicrograph (hematoxylin-eosin stain; magnification, $\times 100$) of nodule (arrows) shows alveolar wall thickening and increased numbers of alveolar lining cells with minimal wall thickening.

using the Kruskal-Wallis test. Shape, marginal characteristics, internal characteristics, and the presence of pleural tag were compared with histopathologic diagnoses by using the Fisher exact test. Although some patients had more than one nodule (53 nodules in 49 patients), we did not perform a generalized estimating equation analysis for data clustering (see Discussion regarding study limitations). A *P* value of less than .05 was considered to indicate a significant difference.

Results

Histologic Diagnoses and Demographic Findings

Of the 53 GGO nodules histopathologically evaluated from 49 (20 men, 29 women; mean age, 54 years; range, 29–78 years) patients, 36 (68%) were diagnosed as BAC (Figs 1–3), four (7%) as adenocarcinoma with predominant BAC component, three (6%) as AAH (Fig 4), and 10 (19%) as nonspecific organizing pneumonia/fibrosis (Figs 5, 6).

Regarding the clinical characteristics of the 49 patients (Table 1), there was no significant difference in either the sex ($P > .99$) or age ($P = .58$) ratio between the BAC or adenocarcinoma with predominant BAC component ($n =$

Figure 5

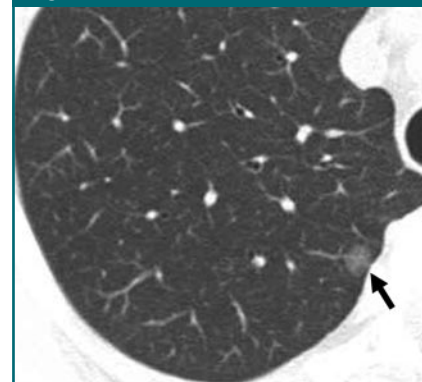


Figure 5: Organizing pneumonia/fibrosis in 50-year-old woman. Transverse lung-window thin-section (2.5-mm-thick) CT scan shows 9-mm round, well-defined GGO nodule (arrow) in right upper lobe. Pathologic wedge resection specimen showed chronic inflammatory cell infiltration in alveolar walls and several tortuous thick-walled vessels with anthracotic pigmentation in peribronchiolar soft tissue and the interlobular septum, suggestive of postinflammatory changes (not shown).

36), AAH ($n = 3$), and nonspecific organizing pneumonia/fibrosis ($n = 10$) patient groups. Multiple nodules were demonstrated in 22% (eight of 36) of BAC or adenocarcinoma with predominant BAC component, 67% (two of

Figure 6

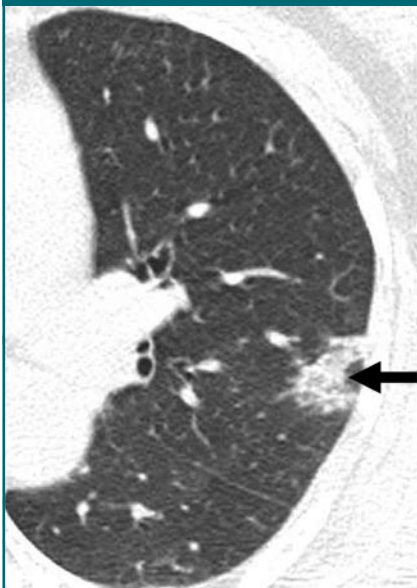


Figure 6: Organizing pneumonia/fibrosis in 51-year-old woman. Transverse lung-window thin-section (1.25-mm-thick) CT scan of right upper lobar bronchus shows 18-mm rectangular GGO nodule with concave margin (arrow) laterally in left upper lobe. Pathologic wedge resection specimen showed alveolar wall thickening owing to inflammation and loose fibrosis, and intra-alveolar inflammatory exudate. Interlobular septal thickening with edema and fibrosis, patchy interstitial lymphoid aggregations with occasional germinal center formation, and pleural puckering with fibrosis were also seen (not shown).

three) of AAH, and 20% (two of 10) of nonspecific fibrosis or organizing pneumonia patients ($P = .21$). Ten (20%) of 49 patients had symptoms such as chest pain, cough, or blood-tinged sputum; nine (90%) of these 10 had BAC or adenocarcinoma with predominant BAC component. However, these results showed no significant difference between the disease groups ($P = .19$). Smoking history ($P = .82$) and history of other prior malignancy ($P = .16$) were also not different between these groups.

Five patients had a previous malignant tumor history; nasopharyngeal cancer in two and rectal cancer, thyroid papillary carcinoma, and thigh liposarcoma in one each. The two patients with BAC had previous history of nasopharyngeal cancer. The GGO nodules were identified on CT scans in 10 patients who underwent chest CT for respiratory symptoms, in 32 patients who underwent lung cancer screening CT, and incidentally in seven patients without pulmonary symptoms who underwent chest CT for other reasons. Positron emission tomography scans, performed in 24 (49%) of 49 patients, demonstrated negative results for malignancy in all patients. Percutaneous needle aspiration biopsy was performed in four patients resulting in final diagnoses of BAC in three and nonspecific fibrosis or organizing pneumonia in one. Biopsy specimens showed positive results for

BAC in only one (25%) of these four patients.

Thin-Section CT Findings

On serial CT studies, which were available in all patients (follow-up range, 1–78 months; mean, 10 months) prior to histopathologic examination, nodules showed an increase in size of more than 5 mm in diameter in two (over a follow-up period of 2 and 72 months, respectively), an increase of up to 5 mm in five (over a follow-up period of 20 months; range, 4–46 months), and no change in 46 patients. The nodules that showed a size increase of more than 5 mm was confirmed as a BAC in one and a chronic inflammation in the other. All lesions that showed a slight size increase (≥ 5 mm) were due to BAC.

The mean values (Table 2) of the maximum diameter \pm standard deviation of GGO nodules were 13 mm \pm 6.9 for BAC or adenocarcinoma with predominant BAC component, 8 mm \pm 3.8 for AAH, and 12 mm \pm 6.7 for nonspecific fibrosis or organizing pneumonia patients ($P \geq .99$). The morphologic characteristics of nodules in terms of shape, marginal characteristics, internal characteristics, and presence of pleural tag were not significantly different between BAC or adenocarcinoma with predominant BAC component, AAH, and nonspecific fibrosis or organizing pneumonia groups. Mean CT attenuation values were -499 HU \pm 171.6 (range, -103 to -775 HU) for BAC and adenocarcinoma with predominant BAC component, -667.3 HU \pm 62.1 (range, -615 to -736 HU) for AAH, and -554.6 HU \pm 165.2 (range, -258 to -792 HU) for nonspecific fibrosis or organizing pneumonia ($P > .99$).

Thin-Section CT–Pathologic Comparisons

Both AAH and BAC showed a replacing growth pattern along the alveolar lining, with no destruction of alveolar walls (Figs 1–4). However, AAH usually had more air spaces and fewer cellular components than did BAC. A polygonal shape (25%, 10 of 40) in BAC or adeno-

Table 1

Patient Demographics

Characteristic	BAC or Adenocarcinoma (n = 36)	AAH (n = 3)	Fibrosis/Organizing Pneumonia (n = 10)	P Value
Sex ratio (M:F)	15:21	1:2	4:6	$>.99^*$
Age (y) [†]	54 \pm 11.4	54 \pm 4.6	54 \pm 8.0	.58 [‡]
Multiplicity	8/36 (22)	2/3 (67)	2/10 (20)	.21*
Positive symptom	9/36 (25)	1/3 (33)	0/10 (0)	.19*
Smoker	8/36 (22)	1/3 (33)	3/10 (30)	.82*
Cancer history	2/36 (6)	1/3 (33)	2/10 (20)	.16*

Note.—Except where indicated, data are numbers of patients, and numbers in parentheses are percentages.

* Fisher exact test.

[†] Data are mean \pm standard deviation.

[‡] Kruskal-Wallis test.

carcinoma with predominant BAC component was associated with fibrosis in the tumor or emphysematous parenchyma. A lobulated or spiculated margin (45%, 18 of 40) in BAC or adenocarcinoma with predominant BAC component corresponded histologically to an area of irregular fibrosis within tumors or an infiltrative tumor growth pattern. A pleural tag (20%, eight of 40) was caused by fibrotic bands usually associated with juxtacatricial pleural retraction.

The main histopathologic feature of organizing pneumonia/fibrosis was the presence of polypoid plugs of loose fibroblastic tissue within alveoli and distal small airways, associated with a variable degree of interstitial and alveolar infiltration by mononuclear cells and foamy macrophages. GGO in organizing pneumonia/fibrosis histologically represented areas of interstitial thickening with fibrosis and chronic inflammatory cell infiltration, deposition of some intra-alveolar polypoid granulation tissue, collapse of airspaces, or contraction of an injured lung (Figs 5, 6).

A polygonal shape (two of 10, 20%) was caused by buds of granulation tissue in the distal airspaces, which simulated apparent septal thickening and contributed to a coarse reticular pattern, even though it was not associated histologically with interlobular septal thickening (Fig 6). A lobulated or spiculated margin (three of 10, 30%) corresponded histologically to areas of organizing exudate accumulation in perilobular alveoli. A pleural tag (one of 10, 10%) was caused by peribronchiolar inflammation and focal areas of linear atelectasis.

Nodal Status and Follow-up Evaluation in Patients with BAC or Adenocarcinoma with Predominant BAC Component

Of 33 patients with single or multiple BACs, 21 patients underwent thoracotomy for curative resection. Three patients with single or multiple adenocarcinomas with predominant BAC component also underwent thoracotomy. None of these 24 patients had nodal metastasis in the hilum or mediastinum (all had no disease).

Table 2

Morphologic Features of GGO Nodules at Thin-Section CT

Characteristic	BAC or Adenocarcinoma (n = 40)	AAH (n = 3)	Fibrosis/Organizing Pneumonia (n = 10)	P Value
Nodule size (mm)*	13 ± 6.9	8 ± 3.8	12 ± 6.7	>.99 [†]
Shape				.20 [‡]
Round	21/40 (53)	3/3 (100)	6/10 (60)	
Oval	9/40 (23)	0/3 (0)	2/10 (20)	
Polygonal	10/40 (25)	0/3 (0)	2/10 (20)	
Margin				>.99 [‡]
Smooth	22/40 (55)	3/3 (100)	7/10 (70)	
Lobulated	10/40 (25)	0/3 (0)	3/10 (30)	
Spiculated	2/40 (5)	0/3 (0)	0/10 (0)	
Lobulated and spiculated	6/40 (15)	0/3 (0)	0/10 (0)	
Internal characteristics				
Solid	3/40 (8)	0/3 (0)	0/10 (0)	>.99 [‡]
Bubble	13/40 (33)	0/3 (0)	0/10 (0)	>.99 [‡]
Pleural tag	8/40 (20)	0/3 (0)	1/10 (10)	>.99 [‡]
Attenuation value (HU)	499 ± 171.6	667 ± 62.1	555 ± 165.2	>.99 [‡]

Note.—Except where indicated, data are numbers of nodules, and numbers in parentheses are percentages.

* Data are mean ± standard deviation.

[†] Kruskal-Wallis test.

[‡] Fisher exact test.

Of 36 patients with BAC or adenocarcinoma with predominant BAC component, 27 were followed up (range, 1–65 months; mean, 16.8 months) with clinical surveillance and CT. Of these 27, 23 had a single nodule, and four had multiple nodules. Patients in whom a single nodule was resected had no evidence of recurrent disease. Two patients with multiple (total 12) nodules, in whom two and three nodules were respectively resected, had same-sized remaining nodules over their respective follow-ups (11 and 17 months). Two patients with multiple (total 18) nodules, in whom one nodule per patient was resected, also had same-sized remaining nodules over follow-up (range, 4–6 months). One patient who had multiple heavy burden of GGO nodules (one of these GGO nodules was confirmed as BAC in wedge resection), received postoperative chemotherapy.

None of the 27 patients with BAC or adenocarcinoma with predominant BAC component died of the disease over the average follow-up period of 17 months (range, 1–65 months).

Discussion

In a study by Nakata et al (8), 28 nodules with pure GGO proved to be BAC (n = 17), AAH (n = 8), or adenocarcinoma (n = 3). However, according to another report (6), of 10 pure GGO nodules at biopsy, five were diagnosed as BAC or adenocarcinoma with mixed cellularity, three as pulmonary lymphoproliferative disease, one as AAH, and one as a fibrotic lesion. Overall, the histologic diagnoses of GGO nodules in our study were 75% (40 of 53 nodules) BAC or adenocarcinoma with predominant BAC component, 6% (three of 53) AAH, and 19% (10 of 53) nonspecific fibrosis or organizing pneumonia. Although the literature shows that lymphoproliferative disease, particularly bronchus-associated lymphoid tissue lymphoma, might appear as a pure GGO nodule, we did not identify a single case manifesting as a GGO nodule.

A number of studies have tried to identify discriminative imaging findings for each disease. Nakata et al (8) reported that GGOs of 10 mm or more in diameter or a solid component within

GGO are informative signs of malignancy, whereas AAH lesions often appear as pure GGO of less than 10 mm in diameter. However, other authors (5,11) have reported cases of AAH larger than 10 mm in diameter, as was observed in one of our three cases. Therefore, the lesion size criterion alone cannot differentiate between BAC and AAH.

Kishi et al (12) reported that a diagnosis of multiple AAHs or BACs should be considered when numerous small, well-defined, and uniform GGO nodules are observed at thin-section CT. However, in our study, multiple GGO nodules were also noted in patients with organizing pneumonia/fibrosis (20%, two of 10), BAC or adenocarcinoma with predominant BAC component (22%, eight of 36), and AAH (67%, two of three).

Furuya et al (13) suggested that analyses of the marginal characteristics of a small pulmonary nodule are useful for determining their nature and reflect their underlying pathologic characteristics. They asserted that a tentacled or polygonal margin is indicative of a benign inflammatory nodule in up to 80% of pulmonary nodules. Histopathologic correlations showed that tentacled or polygonal margins corresponded to areas of fibrosis, dense infiltration by inflammatory cells, collapsed alveoli, or intra-alveolar exudate organization. Retraction of an affected lobule associated with a nodular lesion, in contrast with intact adjacent lobules, causes a concave margin. However, in our study, no significant morphologic differences were observed between BAC or adenocarcinoma with predominant BAC component, AAH, and organizing pneumonia/fibrosis GGO nodules.

By using a description of the CT findings of focal organizing pneumonia, Yang et al (7) proposed that a GGO nodule with an oval or polygonal appearance (especially when the lesion is associated with satellite nodules at CT) suggests a benign nature. However, because the marginal and morphologic characteristics (polygonal shapes of GGO nodules) are not specific findings of any of these diseases, it is very diffi-

cult to differentiate any particular disease from the others.

GGO in BAC represents lepidic tumor growth. However, in a thin-section CT-pathologic correlative study, GGO areas in BAC or adenocarcinoma with predominant BAC component did not histopathologically denote pure lepidic tumor growth areas (14). The GGO component of BACs can be caused by the papillary overgrowth of tumor cells into alveoli, mucin, nonspecific interstitial fibrosis, associated acute pneumonia or respiratory bronchiolitis, or peritumoral hemorrhage (14). Therefore, a polygonal shape and lobulated or spiculated margin can be seen, histologically caused by irregular interstitial fibrosis or an infiltrative tumor growth. Pleural tags are caused by fibrotic bands, associated with juxta-cicatricial pleural retraction (15-17).

In organizing pneumonia/fibrosis, a polygonal shape and a lobulated or spiculated margin are caused by granulation tissues in distal airspaces aligning in a linear manner, thus simulating septal thickening and contributing to a coarse reticular pattern with or without interlobular septal thickening. Pleural tags represent areas of peribronchiolar inflammation and linear atelectasis (7,18,19). Although small in number, in our study, three AAHs appeared as round GGO nodules with a smooth margin without lobulation or spiculation. Thus, the presence of a polygonal shape or lobulated or spiculated margin may preclude the diagnosis of AAH.

Because of difficulties associated with the preoperative or even intraoperative histopathologic diagnoses of small GGO nodules, wide-wedge resection or segmentectomy in combination with intraoperative lavage cytology should be recommended as a safe and minimally invasive method for the diagnosis of GGO nodules (6). Because patients with BAC or adenocarcinoma with predominant BAC component and a GGO nodule have a good prognosis, wedge resection is recommended rather than lobectomy (9,20).

In our study, none of the 24 patients who underwent lobectomy and lymph node dissection had metastatic hilar or

mediastinal lymph nodes. In addition, none of the patients with BAC or adenocarcinoma with predominant BAC component died of the disease. Therefore, limited resection surgery can be recommended in patients with BAC or adenocarcinoma with predominant BAC component and GGO nodules.

Several other studies (21-23) have also suggested that thoracoscopic limited resection for single GGO lesions selected by thin-section CT is valid. A multiple appearance does not imply lower chances of survival. Asamura et al (21) suggested that GGO lesions should be interpreted as surgical candidacy even when a patient has multiple lesions, under the stipulation that the patient has reserved lung parenchymal volume. Moreover, surgical intervention should be followed-up with CT evaluations at proper intervals (3-6 months).

Our study is limited by selection bias. Although we included consecutive patients who underwent surgery or surgical biopsy for lesions appearing as pure GGO nodules, not all patients with a GGO nodule underwent histopathologic confirmation. This may explain why, when compared with previous reports (6,8), our study contains a relatively small percentage of AAH (6%) and no cases of lymphoproliferative malignancy. However, in this study, we tried selectively to include patients with a pure GGO nodule ($\leq 5\%$ of solid component). Another possible limitation is data clustering because we included multiple nodules per patient. However, we did not do a generalized estimating equation analysis to address this, since some literature favors a multiclonal origin of each nodule when BACs are multifocal, indicating that these nodules are not related, but are independent (24,25).

In conclusion, about 75% of pure persistent pulmonary GGO nodules turn out to be BAC or adenocarcinoma with predominant BAC component, and these do not manifest distinguishing morphologic features on thin-section CT images that allow their differentiation from other GGO nodules with different histopathologic diagnoses.

References

- Henschke CI, Yankelevitz DF, Mirtcheva R, McGuinness G, McCauley D, Miettinen OS. CT screening for lung cancer: frequency and significance of part-solid and nonsolid nodules. *AJR Am J Roentgenol* 2002;178:1053-1057.
- Ko JP. Lung nodule detection and characterization with multi-slice CT. *J Thorac Imaging* 2005;20:196-209.
- Kitamura H, Kameda Y, Nakamura N, et al. Atypical adenomatous hyperplasia and bronchoalveolar lung carcinoma: analysis by morphometry and the expressions of p53 and carcinoembryonic antigen. *Am J Surg Pathol* 1996;20:553-562.
- Nomori H, Ohtsuka T, Naruke T, Suemasu K. Differentiating between atypical adenomatous hyperplasia and bronchoalveolar carcinoma using the computed tomography number histogram. *Ann Thorac Surg* 2003;76:867-871.
- Kawakami S, Sone S, Takashima S, et al. Atypical adenomatous hyperplasia of the lung: correlation between high-resolution CT findings and histopathologic features. *Eur Radiol* 2001;11:811-814.
- Kodama K, Higashiyama M, Yokouchi H, et al. Natural history of pure ground-glass opacity after long-term follow-up of more than 2 years. *Ann Thorac Surg* 2002;73:386-392.
- Yang PS, Lee KS, Han J, Kim EA, Kim TS, Choo IW. Focal organizing pneumonia: CT and pathologic findings. *J Korean Med Sci* 2001;16:573-578.
- Nakata M, Saeki H, Takata I, et al. Focal ground-glass opacity detected by low-dose helical CT. *Chest* 2002;121:1464-1467.
- Roberts PF, Straznicka M, Lara PN, et al. Resection of multifocal non-small cell lung cancer when the bronchoalveolar subtype is involved. *J Thorac Cardiovasc Surg* 2003;126:1597-1602.
- Beasley MB, Brambilla E, Travis WD. The 2004 World Health Organization classification of lung tumors. *Semin Roentgenol* 2005;40:90-97.
- Park CM, Goo JM, Lee HJ, et al. CT findings of atypical adenomatous hyperplasia in the lung. *Korean J Radiol* 2006;7:80-86.
- Kishi K, Homma S, Kurosaki A, Tanaka S, Matsushita H, Nakata K. Multiple atypical adenomatous hyperplasia with synchronous multiple primary bronchoalveolar carcinomas. *Intern Med* 2002;41:474-477.
- Furuya K, Murayama S, Soeda H, et al. New classification of small pulmonary nodules by margin characteristics on high-resolution CT. *Acta Radiol* 1999;40:496-504.
- Vazquez MF, Flieder DB. Small peripheral glandular lesions detected by screening CT for lung cancer: a diagnostic dilemma for the pathologist. *Radiol Clin North Am* 2000;38:579-589.
- Zwirewich CV, Vedral S, Miller RR, Muller NL. Solitary pulmonary nodule: high-resolution CT and radiologic-pathologic correlation. *Radiology* 1991;179:469-476.
- Nakajima R, Yokose T, Kakinuma R, Nagai K, Nishiwaki Y, Ochiai A. Localized pure ground-glass opacity on high-resolution CT: histologic characteristics. *J Comput Assist Tomogr* 2002;26:323-329.
- Gaeta M, Barone M, Caruso R, Bartiromo G, Pandolfo I. CT-pathologic correlation in nodular bronchoalveolar carcinoma. *J Comput Assist Tomogr* 1994;18:229-232.
- Ujita M, Renzoni EA, Veeraraghavan S, Wells AU, Hansell DM. Organizing pneumonia: perilobular pattern at thin-section CT. *Radiology* 2004;232:757-761.
- Chen SW, Price J. Focal organizing pneumonia mimicking small peripheral lung adenocarcinoma on CT scans. *Australas Radiol* 1998;42:360-363.
- Nakata M, Sawada S, Saeki H, et al. Prospective study of thorascopic limited resection for ground-glass opacity selected by computed tomography. *Ann Thorac Surg* 2003;75:1601-1605.
- Asamura H, Suzuki K, Watanabe S, Matsuno Y, Maeshima A, Tsuchiya R. A clinicopathological study of resected subcentimeter lung cancers: a favorable prognosis for ground-glass opacity lesions. *Ann Thorac Surg* 2003;76:1016-1022.
- Ohtsuka T, Watanabe K, Kaji M, Naruke T, Suemasu K. A clinicopathological study of resected pulmonary nodules with focal pure ground-glass opacity. *Eur J Cardiothorac Surg* 2006;30:160-163.
- Watanabe S, Watanabe T, Arai K, Kasai T, Haratake J, Urayama H. Results of wedge resection for focal bronchoalveolar carcinoma showing pure ground-glass attenuation on computed tomography. *Ann Thorac Surg* 2002;73:1071-1075.
- Barsky SH, Grossman DA, Ho J, Holmes EC. The multifocality of bronchoalveolar lung carcinoma: evidence and implications of a multiclonal origin. *Mod Pathol* 1994;7:633-640.
- Nanki N, Fujita J, Hojo S, et al. Evaluation of the clonality of multilobar bronchoalveolar carcinoma of the lung: case report. *Am J Clin Oncol* 2002;25:291-295.